

Thermal Management Design and Key Technology Validation for PandaX Underground Experiment

Tao Zhang^{a,b,c,d}, Jianglei Liu^{a,b,c,d}, Yang Liu^b, Weihao Wu^{b,d}, Binbin Yan^{a,*},
Zhou Wang^{a,b,c,d,**}, Zhizhen Zhou^b

^a*New Cornerstone Science Laboratory, Tsung-Dao Lee Institute, Shanghai Jiao Tong University, Shanghai, 201210, China*

^b*School of Physics and Astronomy, Shanghai Jiao Tong University, Key Laboratory for Particle Astrophysics and Cosmology (MoE), Shanghai Key Laboratory for Particle Physics and Cosmology, Shanghai, 200240, China*

^c*Shanghai Jiao Tong University Sichuan Research Institute, Chengdu, 610000, Sichuan, China*

^d*Jinping Deep Underground Frontier Science and Dark Matter Key Laboratory of Sichuan Province,*

Abstract

The scale of liquid xenon experiments for rare events searching is expanding, which is planned even to fifty tons level. The detector and distillation tower require a reliable cooling source with large cooling power at liquid xenon temperature range. Pulse tube refrigerators and GM refrigerators, which were widely used in previous detectors, have the disadvantages of small cooling power, large space occupation, and non-standby mutuality, which become bottlenecks of the experiment scale expansion. In this study, an auto-cascade refrigerator with ethanol coolant is developed, and the heat transfer effect is improved by adopting the concentric shaft heat exchanger and after-pumping heat transfer scheme. The 2.5 kW stable cooling power is obtained at 155 K. Further, the feasibility and key technology of the centralized cooling system of 5 kw at 160 K is discussed. The study can simplify liquid xenon experimental auxiliary devices, which will be helpful for the PandaX-xT experiment scheme and its laboratory infrastructure design.

Keywords: Underground Experiment, Dark Matter, Rare Event, Thermal Management, Auto-Cascade Refrigerator, Centralized Cooling System

*Corresponding author: yanbinbin@sjtu.edu.cn

**Corresponding author: wangzhou0303@sjtu.edu.cn

1. Introduction

Direct detection of dark matter is at the forefront of particle physics experiments, with liquid xenon detectors being the most promising technology. The scale of the detectors has developed from the initial 10kg to the current 10-ton level gradually, such as PandaX[1], XENON[2][3], LZ(LUX)[4]. The scale would reach fifty tons in the long-term plan [5],[6],[7]. Furthermore, the detection target has extended from dark matter to neutrino-less double beta decay events as well [6][8]. To reduce the background from cosmic rays, these experiments must operate in underground laboratories with a long construction period, high cost, and relatively limited space [9]. So, the sizes of the equipment underground, especially surrounding the detector, must be considered in the system design of PandaX-xT.

To improve the detector's sensitivity, the distillation tower for removing Rn and Kr is developed to operate online, and a cold electronic system might be installed inside the detector, increasing the cooling power requirements greatly. The operation temperature of the liquid xenon detector is about 178K. The pulse tube refrigerator (PTR) and GM refrigerators are utilized to supply the cooling power to the detector [10] and the distillation system generally [11]. Liquid nitrogen is used as the powerful auxiliary cooling source for xenon injection and recovery and in emergency conditions. However, the PTR and GM refrigerators are generally oriented to deep temperature refrigeration below 77K, which is expensive and has relatively small cooling power, which does not match the temperature requirements of the liquid xenon detector well. The cooling power allowance is required during design, and the cooling output is adjusted by heating or matching with the thermal load to achieve precise temperature control during operation [10]. In this case, different subsystems, such as the detector and distillation tower, can not share one PTR or GM refrigerator, resulting in the surplus cooling power not supporting each other mutually and the cooling power being wasted. In addition, liquid nitrogen supply is not as convenient as on the ground in China Jinping underground Laboratory (CJPL), so it is infeasible to obtain large cooling power using liquid nitrogen. In conclusion, using a liquid nitrogen-assisted refrigeration scheme based on PTR and GM refrigerators for small-scale liquid xenon experiments is feasible; however, its limited cooling power and low efficiency can not satisfy the experiment's scale expansion requirements.

Therefore, it is necessary to develop thermal management technology for the entire liquid xenon experimental system, adopt a centralized cooling scheme (CCS) and high cooling power refrigeration based on electric energy, improve the efficiency of cold energy utilization, reduce the space and human resource occupation of refrigeration equipment, improve the automation and reliability of the experimental system, and focus on the key task of particle detection.

Section 2 summarizes the requirements of various cooling sources in the PandaX experiment. Section 3 illustrates the design, manufacturing, and performance testing results of the auto-cascade refrigerator (ACR). Section 4 discusses the design and feasibility analysis of the CCS. Section 5 discusses the precision temperature control cold head based on ACR (CHACR). We conclude in section 6.

2. Cooling Source Requirements of PandaX Experiment

In the PandaX experiments, the cooling requirements for a steady-state include the normal operation of the detector and distillation tower, with temperature stability of 178 ± 0.1 K[10],[11]; The transient cooling requirements is pre-cooling of xenon gas and detectors, without temperature stability requirements [5],[12]. The xenon gas recovery stage before the detector ends operation requires room temperature ethanol as the heat source for liquid xenon vaporization [13]. The xenon storage system requires both cooling source and heat source too[5],[12],[14]. Table 1 lists the main technical parameters of the refrigerators selected in the PandaX-4T experiment[10] and the PandaX-xT scheme [6], which need 1 kW and 3.4 kW cooling power, respectively.

Table 1: Cooling power requirements of the PandaX experiments

Experimental device	Cooling power requirement	Refrigerator model	Lowest temperature	Output power	Cooling Power at 178K	Electricity consumption
PandaX-4T Cooling Bus	580 W	RDK-500B (Sumitomo, Japan)	<14 K	80 W @ 30 K	240 W	6.6-6.9 kW
		PT-90 (Cryomech, USA)	32 K	90 W @ 80 K	140 W	4.3 kW
		PC-150 (JEC, Japan)	77 K	170 W @ 165 K	200 W	5.7 kW
PandaX-4T Distillation Tower	400 W 40 W	AL-300 (Cryomech, USA)	25 K	320 W @80 K	500 W	7 kW
		PT-60 (Cryomech, USA)	<30 K	60 W @ 80 K	120 W	2.9 kW
PandaX-xT Cooling Bus	1300 W	AL-600 (Cryomech, USA)	25 K	600 W @ 80 K	950 W	11.5 kW
PandaX-xT Kr Distillation Tower	700 W 115 W	KDE-300SA(Pride,China)	<30 K	250 W @ 77 K	400 W	6.6-6.9 kW
		PT-60 (Cryomech, USA)	<30 K	60 W @ 80 K	120 W	2.9 kW
PandaX-xT Rn Distillation Tower	1300 W	AL-600 (Cryomech, USA)	25 K	600 W @80 K	950 W	11.5 kW

3. Auto-Cascade Refrigeration (ACR)

The CCS requires a centralized high-power refrigeration system or cooling source; one scheme is to use liquid nitrogen as the primary cooling source and then control the temperature [15], which is feasible in ground experiments where liquid nitrogen supply is convenient. However, getting large quantities of liquid nitrogen in CJPL is not convenient, and there is no suitable equipment to produce liquid nitrogen at the CJPL. Considering refrigeration efficiency, using liquid nitrogen to liquify xenon gas is very inefficient due to the huge temperature difference. Electricity is the most convenient and reliable energy at the CJPL, so the electricity-based refrigerator is more suitable for PandaX experiments. The ACR can realize multistage overlapping utilizing a mixture of refrigerant and a compressor and obtain a low temperature below 160 K using an ethanol coolant[16], which facilitates the distribution and management of cooling capacity. The temperature difference of 18 K considers both ACR refrigeration efficiency and the feasibility of CHACR, corresponding to the PandaX 178 K operating temperature.

3.1. ACR Requirements and Design

According to the discussion above, using two ACR units in operation with one as a backup can balance cost-effectiveness and reliability, so the single ACR design cooling power should be more than 2 kW at 160 K.

The working principle of the ACR is shown in figure 1. The ethanol coolant is driven by gear pump A (Model NP1700) from the coolant vessel to the coaxial heat exchanger for cooling, which is also the refrigerator's evaporator. After cooling, the coolant returns to the vessel or directly transfers to the external thermal load. The total volume of the coolant vessel is about 50 L, which is divided by a plate into two parts of 40 L and 10 L with temperature sensors A and B, respectively. There is a gap of about 1 cm between the dividing plate and the inner wall for coolant flow. A filter of 400 meshes is installed at the bottom of the vessel to protect gear pump A, which is driven by a servo motor to adjust the rotary speed continuously, and its rated flow rate is 30 L/min at 2000 r/min. There is an electric heater A between the gear pump A and the coaxial heat exchanger for ice melting. The upper vessel is connected to gear pump B, and the coolant can also be pumped out to the external thermal load. An electric heater B is installed at the output pipeline, which is used for heating mode. The ACR working

principle is described in detail, combined with different operation modes as follows.

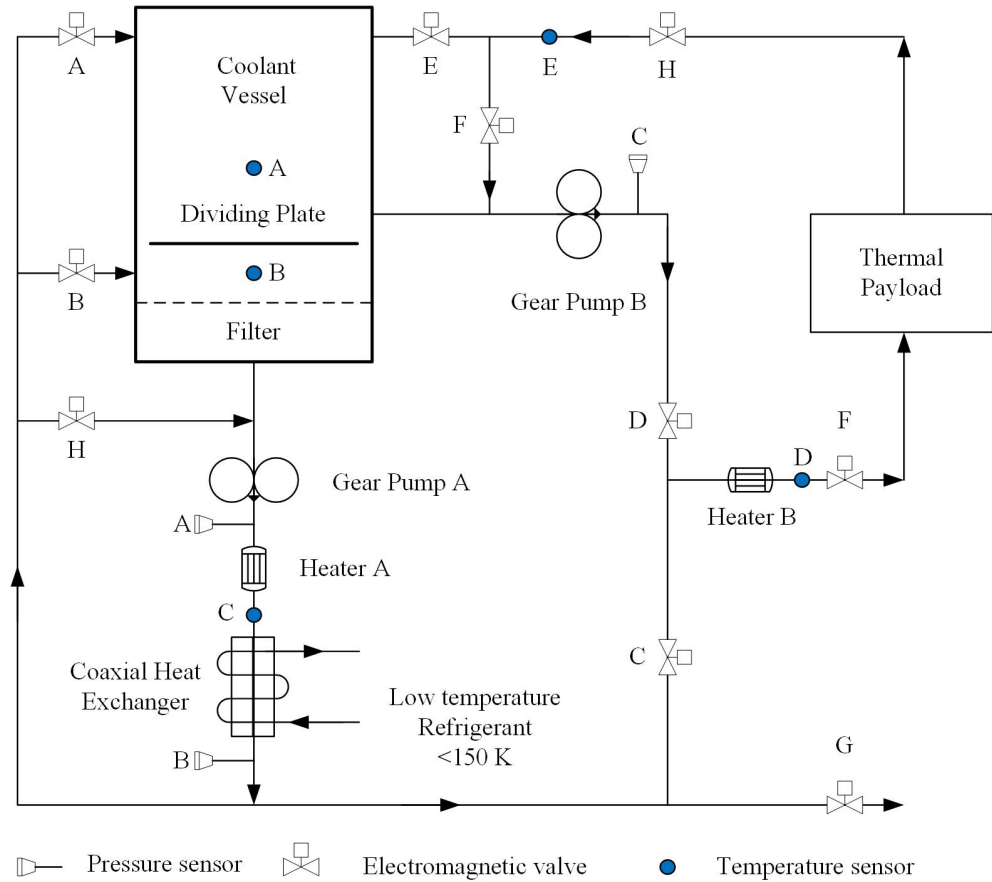


Figure 1: Design principle diagram of ACR

3.1.1. Pre-cooling Mode

It takes about 2 hours to cool the coolant from room temperature to 160 K in the coolant vessel. The ACR can start in this mode for pre-cooling to save time. The rated temperature of the ACR is 160K, so the compressor load is large when the temperature of the coolant flowing through the evaporator is much higher than the rated temperature. The deviation from the rated condition shortens the ACR's life. To solve the problem, it is designed to cool the coolant in the lower secondary refrigerant vessel first, and then the coolant in the upper vessel is cooled gradually.

For example, the ACR started from room temperature with the default operation parameters. In the pre-cooling mode, gear pump A delays starting for a few seconds, and the coolant temperature in the lower vessel determines the flow rate. The flow rate is 5 L/min, 10 L/min, 20 L/min and 30 L/min corresponding to the temperature higher than 273 K, from 223 K to 273 K, from 173 K to 223 K, and lower than 173K, respectively. If the coolant temperature in the lower vessel is above 173 K, the coolant cooled by the evaporator enters the lower vessel via valve B to be further cooled to below 173 K soon because of the smaller volume with the smaller heat capacity of the lower vessel. Then valve A opens, and the cryogenic coolant enters the upper vessel to gradually cool down its internal coolant. Meanwhile, the coolant with a higher temperature in the upper vessel flows into the lower vessel via the gap around the dividing plate and mixes with the low-temperature coolant, causing the temperature to increase. When the temperature rises above 173 K, valve A closes while valve B opens to cool down the lower vessel's coolant preferentially. During the pre-cooling mode, the status of valves A and B switches several times, and the temperature of the upper vessel drops to 173K gradually. Afterward, the stable cooling process starts with valve A opening and valve B closing until the coolant cools to the setting temperature.

3.1.2. Indirect output Mode

This operation mode outputs the cooling coolant to cool down the thermal load, which can be considered an upgraded pre-cooling mode. After the indirect output mode starts, the gear pumps A and B are switched on simultaneously, and the cooling process is consistent with the pre-cooling mode. Valves D and F open while pump B starts, and the thermal load temperature is measured by temperature sensor E after 1 minute. Suppose the temperature difference between sensors A and E is large, more than 30K, for instance. In that case, valve E opens intermittently to reduce the thermal stress, and the temperature difference determines the opening duty rate. The cold coolant in the upper vessel is mixed with the reflux coolant and compressed to the thermal load by gear pump B for cooling. The valve E opens, and valve F closes when the temperature difference between sensors A and E decreases to the setting value, such as 10K, to obtain better heat exchange between the cold coolant in the upper vessel and the thermal load. Thus, the stable cooling output from the vessel is realized for the thermal load. At the same time, the refrigerator also cools the coolant in the vessel,

and valve C opens when the temperatures of the upper vessel and the reflux flow drop to 173 K. Valves A, B, and D, as well as gear pump B, are closed in order to cool down the thermal load directly with the coldest coolant from the evaporator, improving cooling efficiency. In this mode, the stability during the thermal load cooling process is ensured, and the negative influence of the large thermal load with high temperature on the refrigerator life is avoided too.

3.1.3. Direct output Mode

In this mode, the gear pump A starts, and valves A, B, D, F, and H close with valves C and E opening, then the compressor starts cooling after a delay of 1 minute, regardless of the current temperatures of the coolant and thermal load. In this mode, the coldest coolant directly flows to the thermal load to cool it down faster than the indirect out mode. This mode is suitable for rapid cooling requirements.

3.1.4. Deicing Mode

The ethanol in the evaporator has the risk of being solidified when the temperature gets close to or lower than its freezing point, for the designed operating temperature of the refrigerator is low. Once the ethanol solidifies in the evaporator, the heat transfer deteriorates, with the flow resistance increasing and the flow rate decreasing, further worsening the heat transfer. The heat exchanger enters a positive feedback state, rapidly losing its cooling capacity. Two pressure sensors are installed before and after the evaporator for monitoring, and the evaporator is considered to be frozen when the pressure difference exceeds 4 bar, then the ACR enters the deicing mode automatically. When the ACR operates in the indirect output mode, the gear pump B, valves D, and E open, while valves C and F close, and the thermal payload is still cooling by the coolant in the upper vessel. When the ACR operates in pre-cooling mode, the valves A and B close, and the valve H opens. After the deicing mode starts, valves A and B close while valve H opens, and the electric heater of 5kw is switched on, then the flow rate of gear pump A reduces to 2 L/min. The temperature of the heated ethanol is higher than 190 K with a volume of about 5 L in the evaporator. Thus, all the solid ethanol can be melted in 3 minutes at the deicing mode, and the heat exchange function of the evaporator was recovered. The deicing mode exits after 3 minutes automatically, then back to normal operation.

3.1.5. Heating Mode

The PandaX detector vacuum pumping process, the xenon gas recuperation process, and the Photomultiplier Tube (PMT) cryogenic test rewarming process need heat sources. After turning on the heating mode, valves D and F, gear pump B, and electric heater B are activated. Heat is transferred from the ethanol refrigerant to the load until it reaches the set temperature, and the system automatically exits. In heating, the circulating coolant bypass the vessel and evaporator to save energy. The maximum heating temperature is set at 333K, considering the detector's maximum operating temperature and the ethanol's boiling point, corresponding to the ethanol vapor pressure of 47 kPa. Ensuring the sealing of the closed circulation tube line can keep the safety. The cooling process after the heating and vacuuming process of the detector, due to the large temperature difference between the detector and the coolant, the indirect output mode is preferred to ensure the the cooling process smoothly.

3.2. Coolant

It is divided into direct cooling and indirect cooling according to the position relationship of the evaporator and the thermal load during using the cold source. Direct cooling indicates the cold refrigerant exchanges heat with the thermal load in the evaporator directly, whose heat exchange efficiency is higher but lacks of flexibility. Indirect cooling treats the coolant as the intermediate medium, which means the evaporator cools the coolant first, then the cryogenic coolant is pumped to the thermal load for cooling. The so-called coolant was named the second refrigerant, too. Utilizing indirect cooling is convenient for the operation, maintenance, and management of the refrigeration system, as well as the flexible distribution and control of the cooling power. The indirect cooling system can adopt fewer refrigeration units with a larger scale, which is efficient and reliable generally. In the meanwhile, the cooling temperature is stable and reliable because the coolant is also the cold storage medium with large thermal capacity or high thermal inertia. The disadvantage is the refrigeration efficiency reduction compared with the direct cooling for one more heat exchange.

The coolant needs to keep in the liquid phase in the circulation between the evaporator and the thermal load. The anhydrous ethanol is used as the coolant, whose melting point and boiling point are 159 K and 352 K, respectively, and the vapor pressure is 8 kPa at 298 K. The volatility of the ethanol is moderate without stains left after volatilizing so that the pollution

of the experimental equipment is avoided. The disadvantage is that ethanol is flammable, with a flash point of 282 K and a spontaneous combustion point of 695 K; so the tightness of the pipeline is critical. Enhancing the ventilation and installing the ethanol sensor to monitor leakage are required to ensure safety.

In general, melting point is measured in slow heating, cooling and static state [17]. In fact, the flow rate of the ethanol coolant in the ACR is large at highly turbulent state with large cooling rate and temperature gradient, so the liquid flow can still be maintained at subcooling conditions, which has two possible reasons: One is the weak strength of the solid ethanol when the temperature is slightly lower than the melting point, which is similar with the negative correlation of the temperature and the strength of the sea ice and metal materials[18],[19]. Another possibility is that the ethanol coolant is in a fluid-ice state, a mixture of liquid ethanol and tiny solid ethanol crystals [20]. When the temperature is close to or slightly lower than the freezing point, the viscosity of ethanol increases obviously, and the rise in the flow resistance results in a change of the flow characteristics. However, the cooling capacity is increased. In the static test, the ethanol at 150 K in the stainless steel containers has a viscosity similar to the honey. The non-freezing property at the overcooling state is conducive to using ethanol as the coolant, and the lowest output temperature of the ACR is about 150 K in the test.

3.3. Evaporator and Heat Exchanger

The most important technical indicators of a cryogenic refrigerator are the output cooling power and the lowest approachable temperature, which are limited by the performance of the heat exchanger. The increasing cooling power is required to compensate the efficiency reducing of the heat exchanger, and the acquisition cost of the cooling power gets higher as the working temperature decreasing, so the requirement of the heat exchange efficiency is strict [21].

In the previous refrigerator, the coil heat exchanger is arranged as the evaporator in the ethanol coolant vessel, as shown in figure 2A. Refrigerant flows inside the coil while the ethanol coolant is outside. Because of the large vessel section and the small space occupancy of the coil, the flow rate of the coolant is slow during circulation. When the working temperature is much higher than the freezing point of the ethanol, its low viscosity causes the ascendant heat exchange effect. However, the viscosity of the ethanol increases along with the temperature decreasing, and the thickness of the

velocity and temperature boundary layers on the coil surface increases. The flow state tends to change from turbulent to laminar, deteriorating the heat exchange effect. Thus, the lowest output temperature of the refrigerator is limited.

The plate heat exchanger is an efficient and compact heat exchanger composed of a series of parallel thin metal plates with corrugated surfaces, which can be considered as the heat exchanger composed of multiple narrow sub-flow channels in parallel with periodic section changes, resulting in high fluid turbulence and effective heat exchange [22]. However, once the coolant is frozen in a sub-channel at the working condition near the freezing point, the flow resistance of the sub-channel increases, and the flow rate decreases, thus accelerating the solidification process further until the sub-channel is blocked and loses the heat exchange ability, and may leave only one effective sub-channel finally. Thus the effective heat exchange area is much less than the design. So the plate heat exchanger is not suitable.

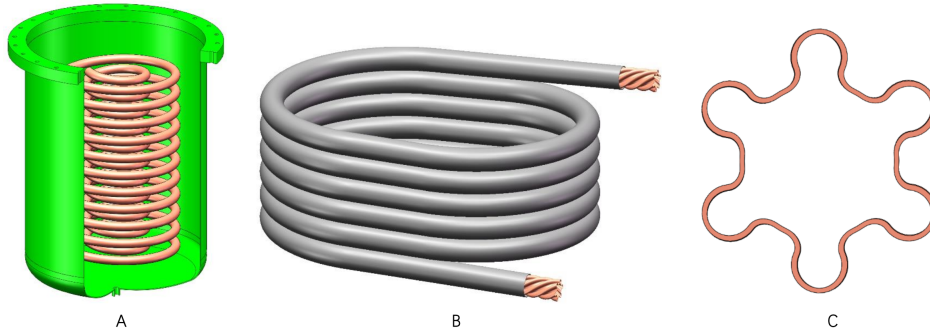


Figure 2: The drawings of coil heat exchanger and coaxial heat exchanger with its cross-section form

The coaxial heat exchanger is a concentric tube consisting of inner and outer tubes of different diameters coiled into round or oblong shapes, as shown in figure 2B. Compared to the coil heat exchanger, shell and tube heat exchanger, and plate heat exchanger, the casing heat exchanger has only one section of the limited flow channel. The cross-section of the inner tube is a star-shaped coolant channel, as shown in figure 2C. Generally, the ethanol coolant is in a highly turbulent state with high heat exchange efficiency due to the uneven and section-changing tube surface. Because the high-speed turbulence flow strongly impacts the tube wall, the solidified micro-crystals are difficult to deposit and grow, and a large amount of coolant solidification

is delayed. Its disadvantage is the relatively large flow resistance [21], and the circulating pump with high-pressure output is required. The output pressure of the gear pump can reach 2 MPa with a maximum suction pressure of 0.09 MPa. The flow resistance of the evaporator increases when the temperature is close to the freezing point of the ethanol. Thus, the gear pump needs to be installed before the evaporator, and the cooling effect of the heat exchanger after the pump fully functions so that the heat exchange reduces the negative impact of the pump heating of the coolant. As a result, the ACR can obtain effective output at lower temperature.

3.4. Circulation Pump

An impeller centrifugal pump is usually used in this kind of refrigerator for its simple structure and high efficiency, whose principle is to transport energy to the fluid medium using the rotating impeller. However, when the viscosity of the medium increases, the shaft power increases, and the efficiency and the flow decreases. The loss of the mechanical energy transfers into heat energy to heat the medium, and the output flow is affected by the outlet pressure obviously [23]. It was found that increasing the power of the centrifugal pump can not improve the output cooling power of the refrigerator in the previous test because its self-heating effect offsets the cooling ability enhanced by increasing the pump power. The gear pump is a positive displacement pump that pressurizes the medium by squeezing the gears, which can transport the medium with a larger viscosity. Its output flow rate is nearly proportional to the rotary speed, almost without being influenced by the outlet pressure [24]. Because the rated temperature of the refrigerator is around the freezing point of ethanol, and the ethanol viscosity is different from the room temperature, the gear pump is chosen as the circulating pump. Furthermore, a servo motor is used to adjust its speed, which takes a soft start to ensure the reliability of the refrigerator; the rotation acceleration is adjustable with a maximum of $5 r/s^2$. At the same time, the pressure sensor is set at the output of the pump to ensure the pressure is below 0.6 MPa or other setting values, and the pump stops with an alarm when the pressure exceeds 0.8 MPa.

3.5. Test Results and Analysis

The ACR dimension is 2 m length, 1.25 m width and 1.9 m height. After the development of the ACR, the electrical heater B in figure 1 is used as the virtual thermal load for testing. The ACR peak power consumption is about 50 kw. The lowest output temperature of the ACR is 151 K with an effective

output power of 2 kw. However, the stability is not enough for condensing the coolant at the heat exchanger. The stable output temperature is 155 K with an output cooling power of 2.5 kW, The cooling power is 3 kW, 3.6 kW, 4 kW, 4.5 kW, 5 kW, 5.6 kW and 6.2 kW, respectively, corresponding to temperatures of 158.5 K, 163 K, 169 K, 177 K, 195 K, 216 K and 233 K. The performance curve is shown in figure 3, the ACR cooling power is much higher than PTR and GM refrigerator which are listed in table 1.

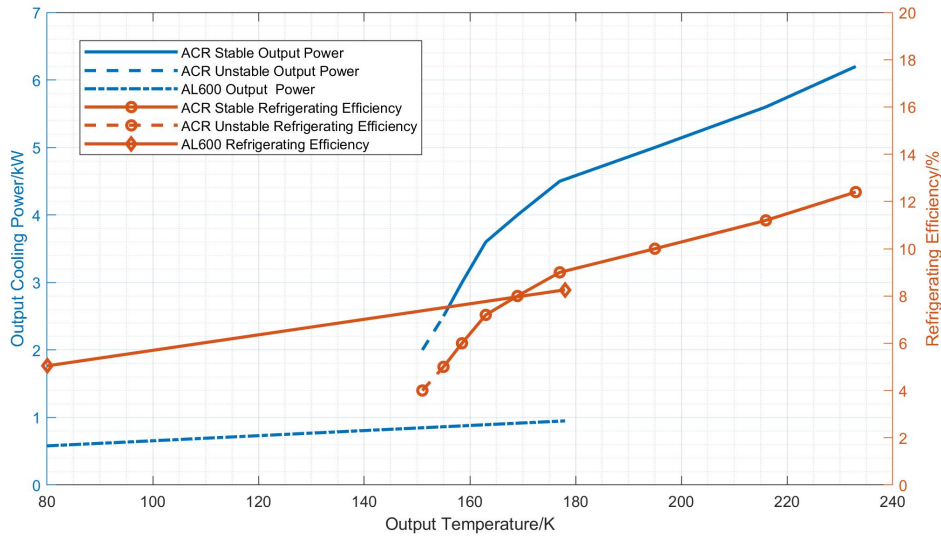


Figure 3: The output performance of ACR and AL600

As shown in figure 3, the refrigeration efficiency of the ACR is near the AL600 refrigerator around 170 K. However, the price per unit of cooling power is significantly lower than AL600. In the applications of PTR and GM refrigerators, the excess cooling power is compensated by electrical heating, and the effective output cooling power is lower than the rated value. The coolant of the ACR has a large heat capacity, and the compressor stops when the coolant is below the setting temperature. The rest of the power of the circulating pump and the control system power is much smaller than the compressor. In the situation where accurate temperature output is required, the precision temperature control method described in section 5 would be used in the ACR to lose a part of the temperature difference, reflecting the decline of refrigeration efficiency. In a word, the refrigeration efficiency of

ACR, PTR, and GM refrigerators can not be compared directly; it is more reasonable to be considered comprehensively in the specific system.

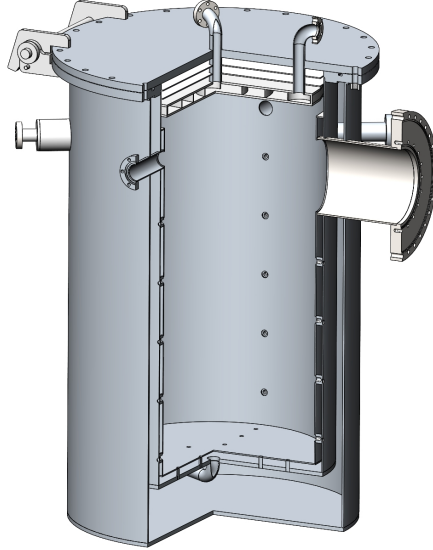


Figure 4: The structure of dewar for PMT cryogenic test

The dewar for the PMT cryogenic test is shown in figure 4, with 450 inner diameters and 735mm height. The total weight of the stainless steel interlayer contact with the coolant is about 80kg. The ACR and dewar are connected with a vacuum-insulated hose with a maximum coolant flow rate of 20 L/min. The temperatures of the gas at the top and bottom of the dewar and the PMTs at different locations are measured, respectively. About 150 minutes is taken to cool down from 300 K to 170 K using the direct output cooling mode, while 40 minutes is spent to return to room temperature using the heating mode, as shown in figure 5. Because the heat transfers from the dewar inner wall to PMT depends on air, the large thermal resistance causes an obvious time delay in the cooling and heating process.

4. Design of Centralized Cooling System (CCS)

As mentioned before, the PandaX experiment requires cooling at multiple locations, CCS is a promising solution. The cold coolant is transported to various thermal payloads by vacuum-insulated pipelines, and the ACR is

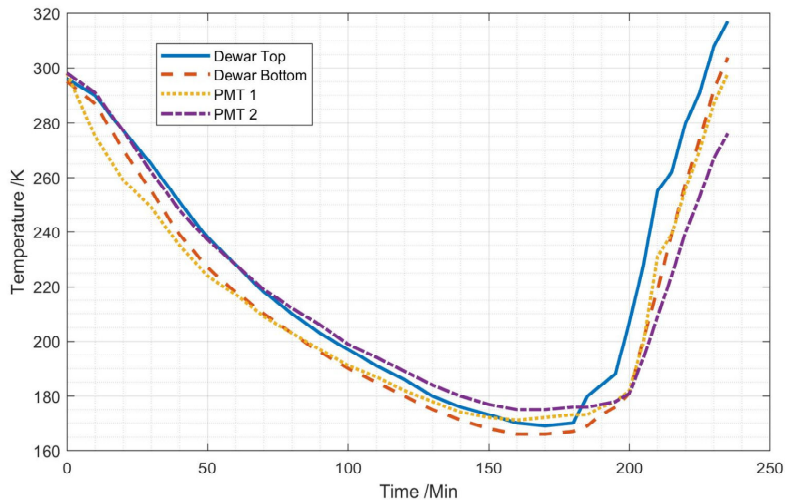


Figure 5: The temperature response of PMT cryogenic test dewar

the operating cold source and liquid nitrogen is back cold source. Similarly, large-scale scientific facilities such as the Beijing Electron-Positron Collider, Large Hadron Collider, China Spallation Neutron Source, and Large Proton Collider have adopted or plan to adopt the CCS with liquid helium temperature zone that provides several kilowatts of cooling power over distances of several kilometers [25].

4.1. Vacuum-insulated Pipeline design

The length and width of the CJPL-II experimental hall, where the PandaX experiment is located, are about 60 m and 14 m, respectively. To ensure the coverage of the cooling supply, the cooling distance is designed to be 100m, which means the total length of the cooling pipeline is about 200 m. The inner diameter of the pipeline is designed to be 50 mm with vacuum insulation and CF flange connection. The maximum flow rate of the pipeline is about 300 L/min by design. Based on the design of a round-trip pipeline temperature difference of 2 K, the maximum cooling power can reach 20 kW, meeting all the cooling requirements of the far future experimental system. Both the inner pipeline and the insulation layer need to pass the helium mass

spectrometry leak detection for safety requirements.

The CCS has about 2000 L of ethanol coolant, which has a large heat capacity and cold storage ability to stabilize the temperature and enhance reliability. The pipeline's heat leakage is about 1 W/m, and each valve's heat leakage is about 1W, so the total heat leakage power is less than 300 W, which is acceptable for the CCS with several kilowatts.

In addition, room-temperature ethanol is needed as a heat source for xenon recuperation [13] and the operation of the distillation tower. Due to the temperature difference being at 140 K, the pipe diameter of 20 mm is enough.

4.2. Multiple Cooling Sources Management

To ensure the reliability of the cooling supply and meet the high-power cooling requirements during stages such as detector pre-cooling and liquid xenon injection, multiple ACRs need to operate simultaneously. A backup ACR that can be put into operation at any time is required, too. Besides the backup ACR, a liquid nitrogen cooling unit is also needed to improve the system's reliability in case of long-time power failure or other extreme conditions. The multiple cooling sources management strategy is shown in figure 6.

Taking PandaX-4T as an example to illustrate, only one ACR can meet all the cooling power requirements for normal operation, the ACR A in figure 6 is running, valves VA and VB opens, valve VC closes, the coolant is circulating. In the meanwhile, The ACR B and the liquid nitrogen cooling unit are connected to the centralized cooling system as thermal loads with valves VD, VE, VG, and VH open, and the coolant circulates slowly to ensure the low-temperature state and ready to output cooling power at any time. If the thermal load is relatively large, like PanaX-xT, only one ACR is not powerful enough; two or more ACRs should run simultaneously, even combined with the liquid nitrogen cooling unit.

There is about 2000 L coolant in the centralized cooling system, and its heat capacity is about 4×10^6 J/K, When the ACRs are shut down, the accumulated cooling capacity can be used to maintain the normal operation of the system. The coolant temperature rose about 1K per 800 seconds for a 5 kW thermal load when all the ACRs stopped briefly. This time is sufficient to start the diesel generator as an emergency backup power source or liquid nitrogen cooling unit. The amount of available liquid nitrogen is about 160 L per container of 200 L, which can provide about 6 kWh of cooling power

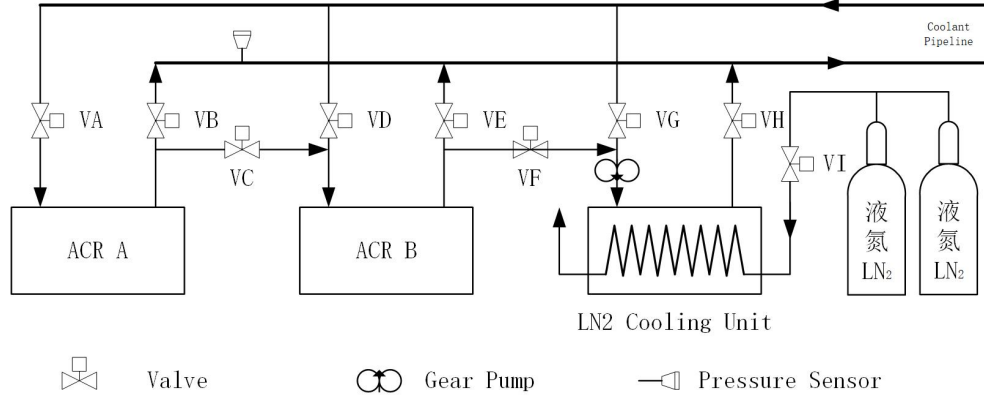


Figure 6: Multiple cooling source management

with the 200 J/g vaporization heat. Unlike PTR and GM refrigerators, the UPS with high power and large capacity is not necessary for ACR; a smaller UPS is sufficient for ACR’s controller and pump, which further saves the cost and space of the experimental system and improves reliability.

4.3. Typical Thermal Load and Access Strategy Analysis

The ACR is relatively inexpensive and has a large cooling power, which can meet most of the cooling requirements of xenon detectors. We will analyze four typical thermal loads, and taking the PandaX-4T detector as an example, provide a simplified thermal management solution to illustrate our design approach and provide reference for future system design.

4.3.1. Thermal Load with Precision Temperature Control

The cooling power requirements are not large when the PandaX detector and the distillation tower are in 178 K steady-state operation. However, the temperature stability requirement is strict, with a tolerance of ± 0.1 K or even ± 0.01 K. The “thermal load A” in figure 7 can be directly connected to the centralized cooling system. The design of the precision temperature control cold head based on the ACR is described in section 5, where the low-temperature coolant is the primary cooling source.

4.3.2. High power thermal load with high temperature

Typical thermal loads include the initial cooling of a large-scale xenon gas storage system and the PandaX detector, which generally start cooling

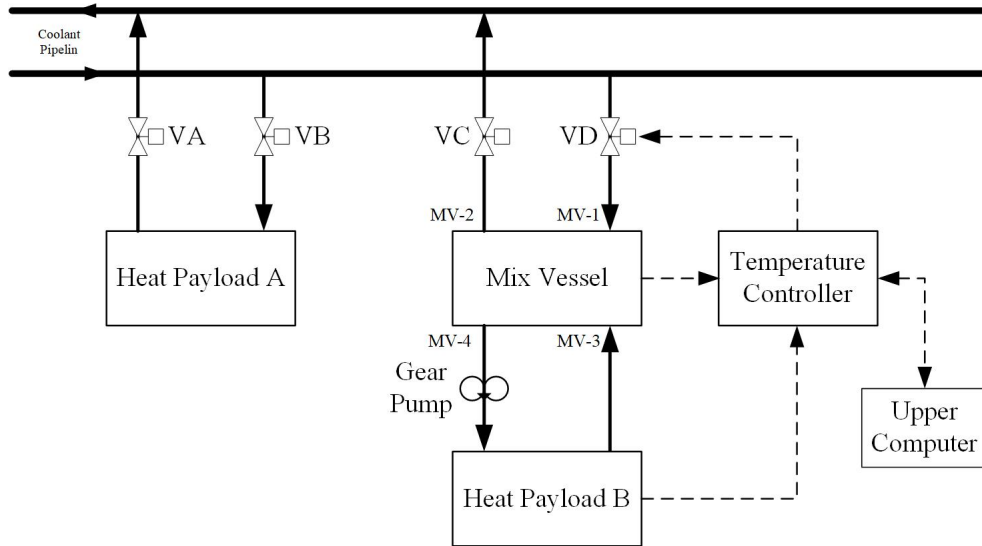


Figure 7: Thermal load access design of CCS

from room temperature to the target temperature over several days. Large cooling power is required regardless of temperature stability. All the ACRs should be in operation. The temperature stability of the coolant needs to be ensured when the other thermal loads with precision temperature control requirements operate in the CCS. A mixer vessel between such thermal loads and the cooling pipeline is useful for these thermal loads, as shown in figure 7.

The mixer is a transition between thermal loads B and the CCS. Functionally, the mixer is similar to the coolant storage tank on a refrigerator. The mixer has four ports for coolant input and output. The coolant driven by the gear pump flows out from port MV-4 at a relatively high flow rate to cool the “thermal load B” and then returns to the mixer through port MV-3. The low-temperature coolant enters the mixer through valve VD and port MV-1 and then returns to the CCS main coolant pipeline through valve VC and port MV-2. Ports MV-1 and MV-3 are close to each other and aligned to achieve a better mixing effect to improve temperature uniformity. The temperature signal is input to the temperature controller, which calculates the opening ratio of the control valve VD based on the upper computer command and the control law to control the coolant in the mixer within the setting temperature range. Though the temperature of the coolant returning to the pipeline through valve VC might be high, the temperature stability

of the cooling supply system can still be ensured when the returning flow rate is low. For example, the Rn adsorption unit requires a cooling source of 180~200 K [15], which can be connected to the CCS through the mixer.

4.3.3. Thermal Load of Xenon Purification Process

This is one of the main thermal loads during the detector's normal operation, which is proportional to the circulation flow rate and the heat exchange coefficient of the circulation system. The heat exchange efficiency is about 97.5% when the circulation flow rate of the PandaX-4T detector is 155 L/min [10], corresponding to the thermal load of approximately 45 W, balanced by the precision temperature-controlled cold head. The thermal load introduced by the circulation and purification process can be calculated for future detectors. As shown in figure 8, if an assistant cooling heat exchanger is added after the cold energy recovering heat exchanger with the ethanal coolant of 163 ± 2 K at the cold side, the purified and cold-recovered gas-liquid mixture is liquefied fully and fed into the detector, thus to avoid the thermal load brought by the xenon circulation and purification process to heat the detector. The specific heat capacity of liquid xenon at 0.2 MPa is about 0.34 kJ/(kg·K).

Taking the PandaX-4T detector as an example for calculation, the cooling power taken from the coolant of 16 K lower than the detector to the detector is up to 60 W. Considering the previous maximum thermal load of 45 W, the cooling power requirement of the other cooling systems of the detector can be reduced by 105 W. The temperature fluctuation of ± 2 K corresponds to a cooling power fluctuation of ± 8 W, and the thermal load fluctuation caused by heat exchange efficiency is small compared to the circulation rate. Changing the circulation flow rate of the coolant can change the heat exchange power of the assistant cooling heat exchanger; thereby, the input cooling power to the detector should be changed. The densities of liquid xenon at 178 K and 163 K are 2854 kg/m^3 and 2956 kg/m^3 , respectively; the difference in the density of 3.6% does not affect the performance of the detector. Therefore, this circulation and purification process supplies adjustable cooling power to the detector, which can reduce the cooling power requirement of the cooling bus, even to cancel the cooling bus.

4.3.4. Thermal Load of Pressure Precision Control of the Detector

During the operation of a dual-phase detector, the significant impact of thermal load is the pressure increase in the detector. The current PandaX

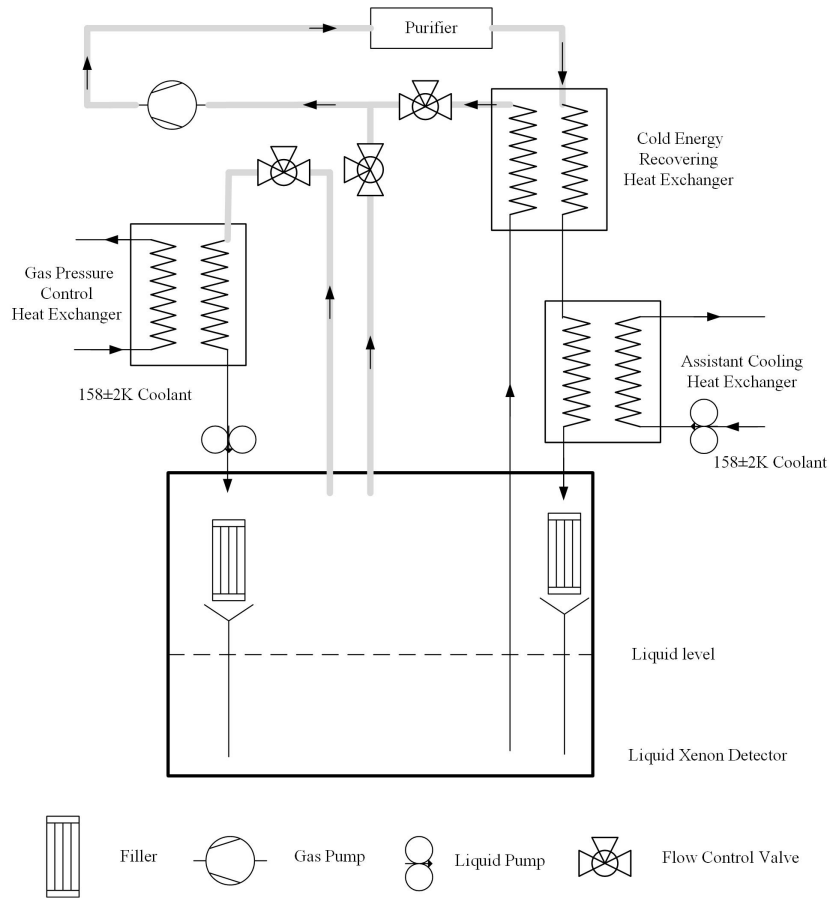


Figure 8: Design diagram of the cooling supplement

cooling systems transfer cooling power from the cold head to the gas xenon through copper cold fingers, and xenon gas is liquefied to reduce the detector pressure. The temperature of the cold head is strictly controlled to ensure the temperature stability in the process [10]. Furthermore, the pressure of the detector can be adjusted by changing the gas phase volume and the total amount of xenon [26]. Therefore, a gas pressure control heat exchanger can be set up based on the convenient supply of coolant, as shown in figure 8, the coolant is at the cold side while the hot side is connected to the gas in the detector via pipeline. It acts as a low-temperature adsorption pump functionally, and the gaseous xenon is absorbed and liquefied, then accumulated to the bottom for gravity and transported to the detector due to

gravity or a gear pump. Considering the temperature gradient of heat transfer, the coolant of 163K ensures the equilibrium pressure of 0.1 MPa on the hot side of the heat exchanger. Compared to the rated operation pressure of 0.2 MPa in the detector, the requirement of the flow resistance of the gas pipeline is not strict for the pressure difference of 0.1 MPa. The flow control valve on the gas pipeline can precisely control the gas flow from the detector to the pressure-controlled heat exchanger, thereby obtaining stable detector pressure. For example, the steady-state operation of PandaX-4T requires a cooling power of about 100 W, while the xenon vaporization heat is about 92 J/g, the pressure in the detector can be balanced by liquefying 1 g/s xenon gas in the heat exchanger. This method is the direct measurement and control of the detector pressure [26], which can control the detector pressure more quickly and accurately and reduce the technical requirements of the temperature control compared to the precise temperature control method using the cold head [10]. The gas phase of the detector can also be connected to the inlet of the gas circulation pump via the gas pipeline and flow control valve, realizing the precise pressure control function of the detector. To ensure the liquid xenon temperature entering the detector is constant, a packing structure similar to a distillation column is added to the return liquid xenon pipeline. The packings are located in the gas phase of the detector, and the liquid xenon with lower temperature exchanges heat and mass with the gas xenon on the surface of the packings; some gas xenon is liquefied and quickly balanced to the equilibrium temperature, then injected into the specified position of the detector by gravity, which can keep the stability of the detector operation without the requirement of the complex temperature control system. The packing acts as an adsorption pump functionally for gaseous xenon.

5. Design of Cold Head based on ACR (CHACR)

The ACR can achieve a temperature of below 160K. However, its operating principles determine the temperature fluctuation of the output is relatively large at the level of ± 2 K, which can not meet the temperature stability requirement of 178 ± 0.1 K for the PandaX experiment system. It is feasible to design and manufacture CHACR with reference to PTR and GM cold heads. The refrigerant flow control based on a flow regulating valve is used as the coarse adjustment, precise adjustment is carried out by electric heating, and the control signal is all from the temperature controller. figure 9

shows the design principle of CHACR. The coolant channels are designed at the top of the copper rod with a diameter of 150mm, and a precision temperature sensor is at the bottom of the copper rod for temperature control, and the temperature is defined as the output temperature of CHACR. The bottom of the copper rod is thermally connected to the cold finger via the thermal adhesive, and the cold finger can cool down the xenon gas in the PandaX detector or the distillation tower directly. For stable thermal load, increasing the cold coolant flow rate can decrease the output temperature of the CHACR and vice versa. As a thermally conductive structure, the copper rod itself has a low-pass filtering effect on temperature fluctuations at the input end, so a sampling frequency of 10Hz is sufficient for the CHACR temperature controller. The coolant flow rate should be operated within 10% to 30% of the full precision electric heating power of the temperature controller, which can balance system efficiency and fast response to transient thermal loads. The cooling power of the AL600 cold head with a 127 mm diameter is about 950 W at 178 K. The CHACR can obtain the same cooling power or more.

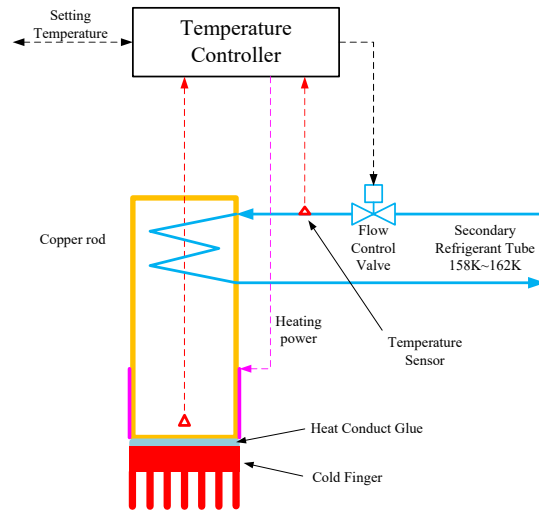


Figure 9: The design principle of the CHACR

6. Conclusion

The developed ACR uses the gear pump to drive ethanol coolant and utilizes the coaxial heat exchanger after the pump to achieve the stable output of 2.5 kW at 155 K, which can meet the temperature and power requirements of the liquid xenon experiments. Further, a centralized cooling system with a precision temperature control cold head based on ACR is designed, which is convenient for distributing cooling capacity to improve the utilization efficiency and reduce the complexity of the auxiliary devices of the liquid xenon experimental system. The technology can be used in the PandaX-xT and provide references for the design and construction of underground laboratory infrastructures.

Acknowledgments

This work was supported by grants from the Ministry of Science and Technology of China (No. 2023YFA1606203, No. 2023YFA1606200), Shanghai Pilot Program for Basic Research — Shanghai Jiao Tong University (No. 21TQ1400218), the Science and Technology Commission of Shanghai Municipality (Grant No.22JC1410100), National Science Foundation of China (No. 12090060, U23B2070). We thank for the support by the Fundamental Research Funds for the Central Universities. We also thank the sponsorship from the Chinese Academy of Sciences Center for Excellence in Particle Physics (CCEPP), Hongwen Foundation in Hong Kong, New Cornerstone Science Foundation, Tencent Foundation in China, and Yangyang Development Fund, and the Yalong River Hydropower Development Company Ltd. for indispensable logistical support and other help. Finally, the authors thank the technical support from Qiangxing LIN of Shanghai SUOFU Co., Ltd. and Yonghuang DENG of Shenzhen Ruixue Refrigeration Equipment Co., Ltd, we have united and cooperated, making a small push for the development of productive force.

References

- [1] H. Zhang, A. Abdukerim, W. Chen, et. al, Dark matter direct search sensitivity of the pandax-4t experiment, *Science China Physics, Mechanics and Astronomy* 62 (3) (2019) 031011. [doi:10.1007/s11433-018-9259-0](https://doi.org/10.1007/s11433-018-9259-0).

- [2] J. Angle, E. Aprile, F. Arneodo, et. al, First results from the xenon10 dark matter experiment at the gran sasso national laboratory, *Physical Review Letters* 100 (2008) 021303. doi:[10.1103/PhysRevLett.100.021303](https://doi.org/10.1103/PhysRevLett.100.021303).
- [3] E. Aprile, J. Aalbers, F. Agostini, et. al, The xenon 1t dark matter experiment, *The European Physical Journal C* 77 (12) (2017) 881. doi:[10.1140/epjc/s10052-017-5326-3](https://doi.org/10.1140/epjc/s10052-017-5326-3).
- [4] D. Akerib, X. Bai, S. Bedikian, et. al, The large underground xenon (lux) experiment, *Nuclear Instruments and Methods in Physics Research A* 704 (2013) 111–126. doi:[10.1016/j.nima.2012.11.135](https://doi.org/10.1016/j.nima.2012.11.135).
- [5] T. Zhang, J. Liu, High purity xenon management and heat management design for hundred tons scale liquid xenon experiment, *Vacuum and Cryogenics* 29 (2) (2023) 200–208. doi:[10.3969/j.issn.1006-7086.2023.02.014](https://doi.org/10.3969/j.issn.1006-7086.2023.02.014).
- [6] A. Abdukerim, Z. Bo, W. Chen, et. al, Pandax-xt, a deep underground multi-ten-tonne liquid xenon observatory, *SCIENCE CHINA*.arXiv:[2402.03596](https://arxiv.org/abs/2402.03596).
- [7] L. Baudis, Darwin/xlzd: A future xenon observatory for dark matter and other rare interactions, *Nuclear Physics B* 1003 (2024) 116473, special Issue of Nobel Symposium 182 on Dark Matter. doi:<https://doi.org/10.1016/j.nuclphysb.2024.116473>.
- [8] K. Ni, Y. Lai, A. Abdusalam, et. al, Searching for neutrino-less double beta decay of ^{136}Xe with pandax-ii liquid xenon detector, *Chinese Physics C* 43 (11) (2009) 113001. doi:[10.1088/1674-1137/43/11/113001](https://doi.org/10.1088/1674-1137/43/11/113001).
- [9] J. Li, X. Ji, W. Haxton, et. al, The second-phase development of the china jinping underground laboratory, *Physics Procedia* 61 (2015) 576–585. doi:[10.1016/j.phpro.2014.12.055](https://doi.org/10.1016/j.phpro.2014.12.055).
- [10] L. Zhao, X. Cui, W. Ma, et. al, The cryogenics and xenon handling system for the pandax-4t experiment, *Journal of Instrumentation* 16 (2021) T06007. doi:[10.1088/1748-0221/16/06/T06007](https://doi.org/10.1088/1748-0221/16/06/T06007).

- [11] R. Yan, Z. Wang, X. Cui, et. al, Pandax-4t cryogenic distillation system for removing krypton from xenon, Review of Scientific Instruments 92 (2021) 123303. [doi:10.1063/5.0065154](https://doi.org/10.1063/5.0065154).
- [12] T. Zhang, J. Liu, Large scale storage of high purity gas with rapid liquefaction and recovery device, Chinese Patent: CN115307050A.
- [13] Z. Wang, W. Ma, T. Zhang, et. al, Design and operation of the pandax-4t high speed ultra-high purity xenon recuperation system, Journal of Instrumentation 17 (2022) T10008. [doi:10.1088/1748-0221/17/10/T10008](https://doi.org/10.1088/1748-0221/17/10/T10008).
- [14] X. Wang, Z. Lei, Y. Ju, et. al, Design, construction and commissioning of the pandax-30t liquid xenon management system, Journal of Instrumentation 18 (05) (2023) P05028. [doi:10.1088/1748-0221/18/05/P05028](https://doi.org/10.1088/1748-0221/18/05/P05028).
- [15] X. Jiang, L. Zhao, S. Wang, et. al, A ln_2 -based cryogenic system prototype for future pandax experiment, Journal of Instrumentation 17 (2022) T07005. [doi:10.1088/1748-0221/17/07/T07005](https://doi.org/10.1088/1748-0221/17/07/T07005).
- [16] T. Zhang, J. Liu, A wide temperature range low-temperature refrigerator, Chinese Patent 202320362287.7.
- [17] P. Bruice, Essential Organic Chemistry 3rd, 2015.
- [18] D. Meng, X. Chen, S. Ji, Prediction and analysis of flexural strength of sea ice based on recurrent neural network, Mechanics in Engineering 44 (3) (2022) 580–589. [doi:10.6052/1000-0879-21-434](https://doi.org/10.6052/1000-0879-21-434).
- [19] T. Li, M. Hassan, K. Kuwana, Performance of secondary aluminum melting: Thermodynamic analysis and plant-site experiments, Energy 31 (2006) 1769–1779. [doi:10.1016/j.energy.2005.08.005](https://doi.org/10.1016/j.energy.2005.08.005).
- [20] X. Shao, C. Wang, Y. Yang, et. al, Screening of sugar alcohols and their binary eutectic mixtures as phase change materials for low-to-medium temperature latent heat storage: Non- isothermal melting and crystallization behaviors, Energy 160 (2018) 1078–1090. [doi:10.1016/j.energy.2018.07.081](https://doi.org/10.1016/j.energy.2018.07.081).

- [21] D. Popov, K. Fikiin, B. Stankov, et. al, Cryogenic heat exchangers for process cooling and renewable energy storage: A review, *Applied Thermal Engineering* 153 (2019) 275–290. [doi:10.1016/j.applthermaleng.2019.02.106](https://doi.org/10.1016/j.applthermaleng.2019.02.106).
- [22] O. Arsenyeva, J. Klemeš, E. Klochock, et. al, The effect of plate size and corrugation pattern on plate heat exchanger performance in specific conditions of steam-air mixture condensation, *Energy* 263 (2023) 125958. [doi:10.1016/j.energy.2022.125958](https://doi.org/10.1016/j.energy.2022.125958).
- [23] L. Zhang, X. Wang, P. Wang, et. al, Optimization of a centrifugal pump to improve hydraulic efficiency and reduce hydro-induced vibration, *Energy* 268 (2023) 126677. [doi:10.1016/j.energy.2023.126677](https://doi.org/10.1016/j.energy.2023.126677).
- [24] A. Josifovic, J. Roberts, J. Corney, et. al, Reducing the environmental impact of hydraulic fracturing through design optimisation of positive displacement pumps, *Energy* 115 (2016) 1216–1233. [doi:10.1016/j.energy.2016.09.016](https://doi.org/10.1016/j.energy.2016.09.016).
- [25] Y. Zhang, G. Wang, Z. Hu, et. al, Review of cryogenic development and advance research in large scientific projects, *Cryogenics* 3 (2016) 17–22. [doi:1000-6516\(2016\)03-0017-06](https://doi.org/10.1016/j.cryogenics.2016.03.001).
- [26] T. Zhang, J. Liu, A pressure precision control device for dual-phase detector, Chinese Patent 202222807631.7.